Site Directed Mutagenesis Maps Interactions that Enhance Cognate and Limit Promiscuous Catalysis by an Alkaline Phosphatase Superfamily Phosphodiesterase

*Helen Wiersma-Koch, Fanny Sunden, and Daniel Herschlag**

Department of Biochemistry, Stanford University, Stanford, CA 94305, USA

Supporting Information

pH dependencies of the monoesterase and diesterase reaction of the NPP mutants.

Part 1: pH dependence of T90S/F91A/L123A/Y205A. Wild-type NPP not only distinguishes between monoester and diester substrates by greater than 200-fold, but it also discriminates between the reaction of $pNPP^{1-}$ and $pNPP^{2-}$ by 72-fold. We asked whether this "minimal" mutant distinguishes between these two reactions. To do so, we performed a pH dependence from pH 4.7 to 8.0 under subsaturating conditions with both Me-pNPP and pNPP (Figure S3A). Me-pNPP has a pK_a of <2 and allows us to determine if there is an enzymatic pK_E in this region (Eq. 1; Scheme 1A). The pK_E is a property of the enzyme so the same pK_E should appear in the pNPP pH dependence. Other pH-dependent rate effects in the pH-rate profile would be expected to arise from differential catalysis of $pNPP^{1-}$ and $pNPP^{2-}$ (Eq. 2; Scheme 1B).

The Me-pNPP pH dependence revealed an acidic limb, as did the pNPP pH dependence (Figure S3A). The ratio of the pNPP and Me-pNPP was fit to equation (3), which was derived from Schemes S1A and S1B and Equations 1 and 2 to eliminate the dependence on the enzymatic pK_E and leave only any dependence on the pK_a of PNPP –i.e., on the relative amount of $pNPP^{2-}$ versus $pNPP^{1-}$ present. The near-indistinguishable observed shapes of the pH-rate profiles, as demonstrated by the near-flat line in Figure S3B, indicates that $pNPP^{2-}$ and $pNPP^{1-}$ react at similar rates. Fitting the pH-dependence of Figure S3B to Eq. 3 gives $(k_{cat}/K_M)'_{pNPP^{1-}}$ = ~5 $M^{-1}s^{-1}$, a value that can be directly compared to the observed k_{cat}/K_M = 5.7 $M^{-1}s^{-1}$ for $pNPP^{2-}$ at the pH plateau [i.e., $(k_{cat}/K_M)'_{pNPP^{2-}}$].

Scheme S1: Kinetic scheme for the reaction of pNPP with T90S/F91A/L123A/Y205A as a function of pH.

A

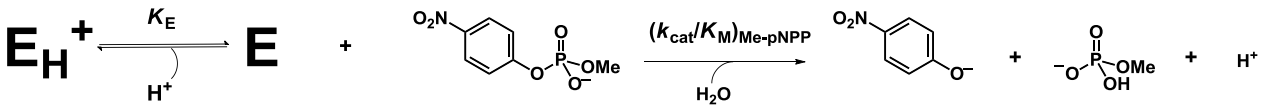

B

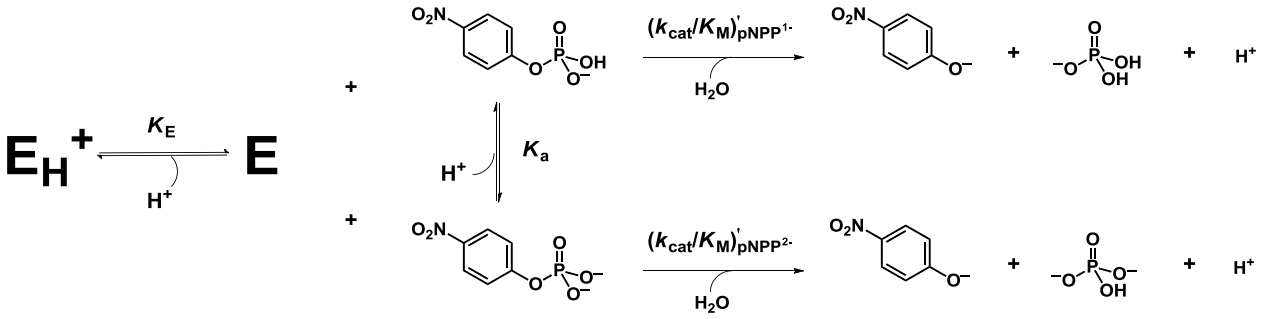

$$(k_{cat}/K_M)_{me-pNPP,obs} = \frac{(k_{cat}/K_M)_{Me-pNPP,obs}}{1+10^{pK_E-pH}} \quad (1)$$

$$(k_{cat}/K_M)_{pNPP,obs} = \left[(k_{cat}/K_M)_{pNPP^{2-}} + \frac{(k_{cat}/K_M)'_{pNPP^{1-}} - (k_{cat}/K_M)'_{pNPP^{2-}}}{1+10^{pH-pK_{a,pNPP}}}\right] \frac{1}{1+10^{pK_E-pH}} \quad (2)$$

$$k_{rel} = \left[(k_{cat}/K_M)_{pNPP^{2-}} + \frac{(k_{cat}/K_M)'_{pNPP^{1-}} - (k_{cat}/K_M)'_{pNPP^{2-}}}{1+10^{pH-pK_{a,pNPP}}}\right] \frac{1}{(k_{cat}/K_M)_{Me-pNPP,obs}} \quad (3)$$

Part 2: pH dependence of the pNPP reaction with the R′-pocket mutants. To ensure that the rate constants being measured in the R′-pocket mutants corresponded to the reaction of, $pNPP^{2-}$, and

not $pNPP^{1-}$, we determined the pH dependencies with all of the mutants. The pH dependencies showed less than a 2-fold changes between pH 7 – 9, except for the Y205A and T90S/F91A/L123A/y205A mutants, which showed greater scatter, with 4- and 3-fold ranges, respectively (Figure S4). These results confirm that the dianionic form of pNPP preferentially reacts with the mutants over this pH range.

001′-MKIKTGARILALSALTTMMFSASALAKIEEGKLVIWINGDKGYNGLAEVGKKFEKDTGIK

061′-VTVEHPDKLEEKFPQVAATGDGPDIIFWAHDRFGGYAQSGLLAEITPDKAFQDKLYPFTW

121′-DAVRYNGKLIAYPIAVEALSLIYNKDLLPNPPKTWEEIPALDKELKAKGKSALMFNLQEP

181′-YFTWPLIAADGGYAFKYENGKYDIKDVGVDNAGAKAGLTFLVDLIKNKHMNADTDYSIAE

241′-AAFNKGETAMTINGPWAWSNIDTSKVNYGVTVLPTFKGQPSKPFVGVLSAGINAASPNKE

301′-LAKEFLENYLLTDEGLEAVNKDKPLGAVALKSYEEELAKDPRIAATMENAQKGEIMPNIP

361′-QMSAFWYAVRTAVINAASGRQTVDEALKDAQTNSSSNNNNNNNNNNLGIEGRASASTPHA

421′-LLLISIDGLRADMLDRGITPNLSHLAREGVRARWMAPSYPSLTFPNHYTLVTGLRPDHHG

481′-IVHNSMRDPTLGGFWLSKSEAVGDARWWGGEPVWVGVENTGQHAATWSWPGSEAAIKGVR

541′-PSQWRHYQKGVRLDTRVDAVRGWLATDGAQRNRLVTLYFEHVDEAGHDHGPESRQYADAV

601′-RAVDAAIGRLLAGMQRDGTRARTNIIVVSDHGMAEVAPGHAISVEDIAPPQIATAITDGQ

661′-VIGFEPLPGQQAAAEASVLGAHDHYDCWRKAELPARWQYGSHPRIPSLVCQMHEGWDALF

721′-PDKLAKRAQRGTRGSHGYDPALPSMRAVFLAQGPDLAQGKTLPGFDNVDVYALMSRLLGI

781′-PAAPNDGNPATLLPALRMPPAPDARIEGRSAWSHPQFEK

Figure S1. Sequence of the wild-type MBP-NPP$_{Strep}$ construct. In purple is the sequence of MalE, the Maltose Binding Protein. Underlined, in bold green is the N-terminal periplasmic export sequence, which is cleaved during processing, and the MalE polylinker. Underlined, in bold blue are the Factor Xa cleavage sites at the N- and C- termini of *Xanthomonas axonopodis* (pv. citri) NPP, whose sequence is shown in plain black text. Underlined, in bold pink at the C-terminus is the sequence of the StrepII tag used for purification. Within the sequence of NPP, the nucleophilic Thr, of which the methyl group forms part of the R′-pocket, is highlighted in green, the six other R′-pocket residues are highlighted in yellow, and the zinc-ligands are highlighted in red. Residue number prime of the MBP-NPP$_{Strep}$ construct are not equal to residue number used throughout text.

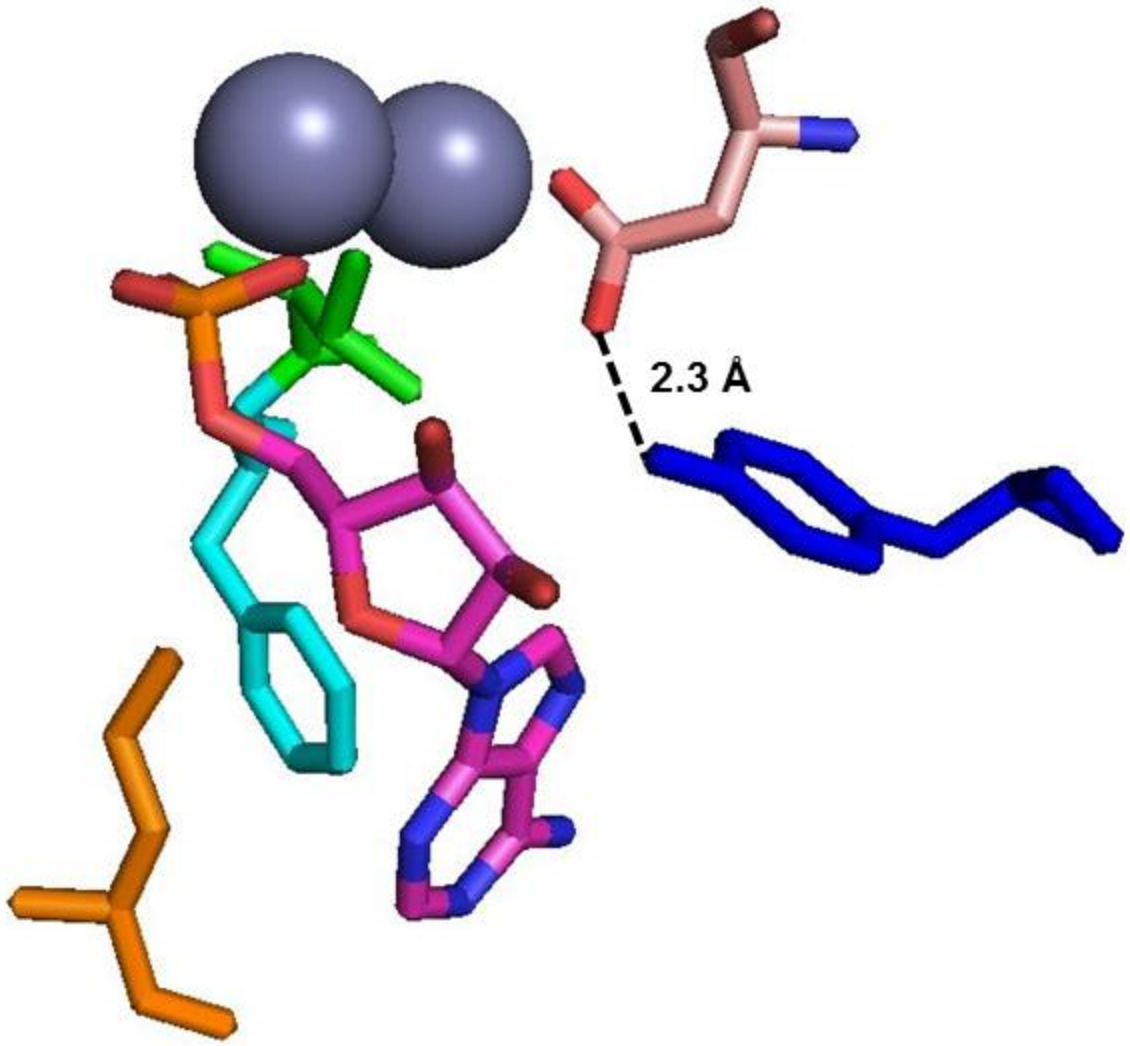

Figure S2. Schematic of the hydrogen bond between Y205 and the Zn^{2+} ligand D54. This hydrogen bond structurally connects Y205 to the active site and may play a small, but significant role in ordering the active site. The positioning of the Zn^{2+} ions (gray), AMP (magenta), T90 (green), F91 (aqua), L123 (orange), Y205 (blue), and D54 (salmon) with respect to each other are from the 2GSU crystal structure.[1]

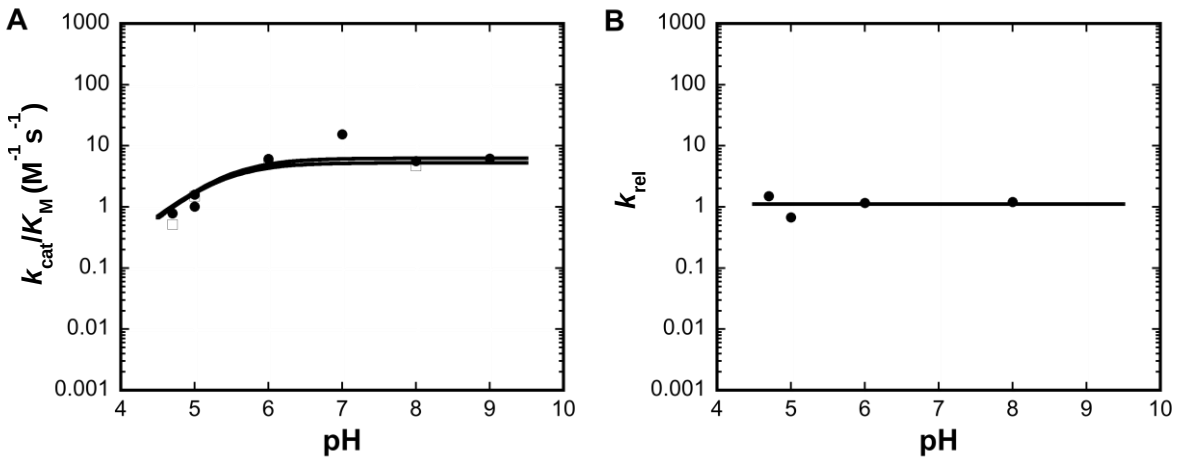

Figure S3. pH dependencies of the T90S/F91A/L123A/Y205A mutant. (A) pH dependence of the pNPP (□, solid line) and Me-pNPP (•, dashed line) reactions. Enzymatic pK_a values of 5.4 and 5.3 were obtained for the pNPP and Me-pNPP reactions, respectively (Eq. 1). (B) T90S/F91A/L123A/Y205A reacts with both with $pNPP^{2-}$ and $pNPP^{1-}$. These results are described by Scheme S1 and Equation S3, derived from Equations S1 and S2. In Equation S3 the observed rate constants for pNPP hydrolysis are normalized by those for Me-pNPP hydrolysis to eliminate effects arising from the enzymatic ionization. The line is a non-linear least squares fit to a model in which NPP reacts with $pNPP^{1-}$ and $pNPP^{2-}$ with a fixed, previously experimentally determined pK_a of 4.79[1] and gives values for k_{cat}/K_M of the $pNPP^{2-}$ and $pNPP^{1-}$ reactions of 5.7 $M^{-1}s^{-1}$ and 5 $M^{-1}s^{-1}$.

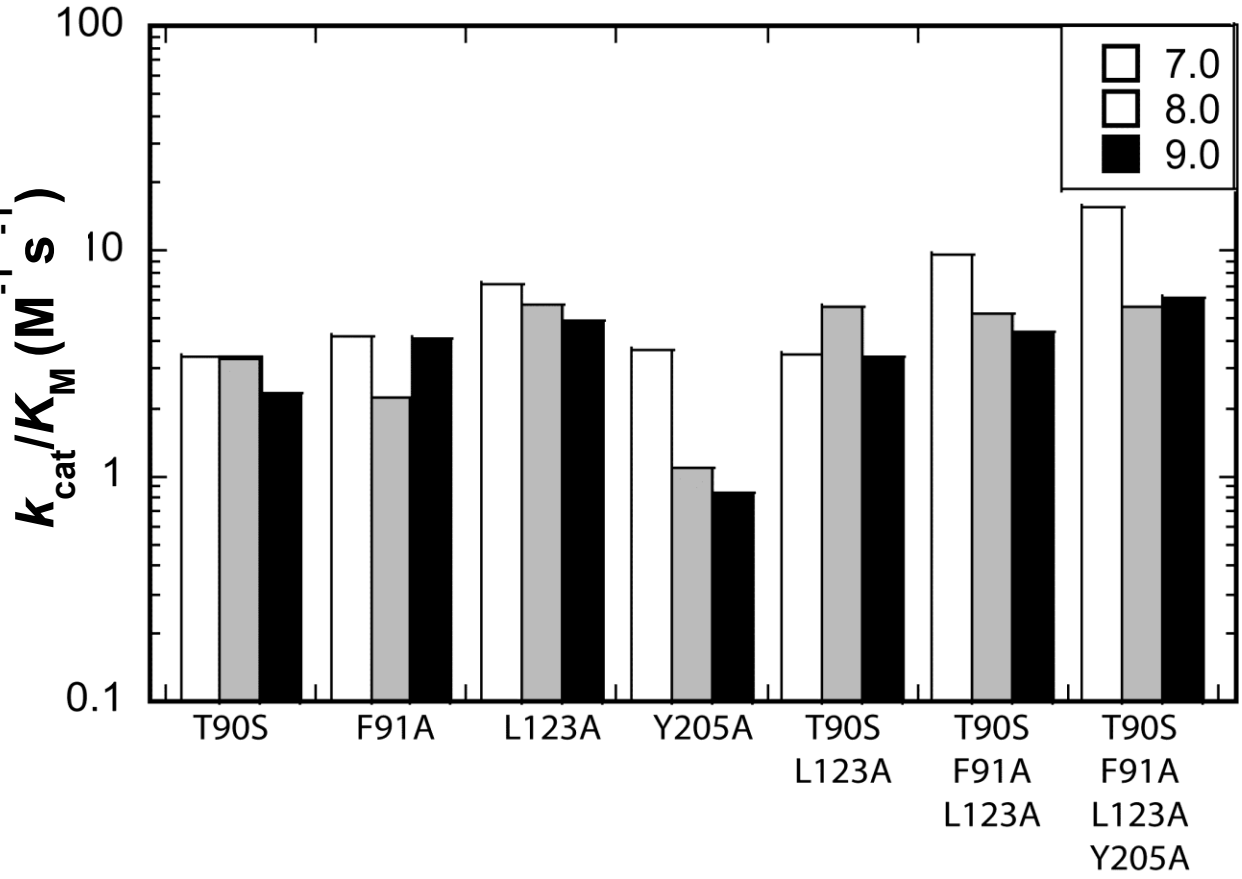

Figure S4. pH dependencies of the pNPP reaction with the R′-pocket mutants from pH 7 – 9. The bar graphs for each mutant shows no more than a 7-fold change (Y205A) in k_{cat}/K_M values over a two log change in pH, indicating that the dianionic form of pNPP is reacting with the mutants at the condition used (pH 8.0) to determine k_{cat}/K_M values for all reactions with all of the mutants – the exception being the pH dependencies of the Me-pNPP and pNPP reactions used to extrapolate the k_{cat}/K_M value of $pNPP^{1-}$ of the quadruple mutant (Figure S3).

REFERENCE:

1. Zalatan, J. G., Fenn, T. D., Brunger, A. T., and Herschlag, D. (2006) Structural and Functional Comparisons of Nucleotide Pyrophosphatase/Phosphodiesterase and Alkaline Phosphatase: Implications for Mechanism and Evolution. *Biochemistry 45*, 9788-9803.